Effect of Forging on Cyclic Hardening Behavior of CW 614 Brass Alloy

R. Mnif,[a] R. Elleuch,[a] K. Elleuch,[a] N. Haddar,[b] and F. Halouani[a]

[a] Laboratoire des Systèmes Electro-Mécanique (LASEM), Ecole Nationale d'Ingénieurs de Sfax, Tunisie

[b] Centre des Matériaux (UMR CNRS 7633), Ecole Nationale Supérieure des Mines de Paris, France

Влияние ковки на циклическое упрочнение латуни CW 614

Р. Мниф[a], Р. Эллюш[a], К. Эллюш[a], Н. Хаддар[б], Ф. Халуани[a]

[a] Лаборатория электромеханических систем, Национальный инженерный институт, Сфакс, Тунис

[б] Центр материаловедения, Национальный горный институт, Париж, Франция

Проведено исследование циклического упрочнения латуни CW 614 на образцах, изготовленных по двум технологиям: промышленная и путем ковки. Для каждого типа образца установлены особенности циклического упрочнения и циклической петли гистерезиса. Представлены результаты анализа процесса разрушения на основе фрактографических исследований.

Ключевые слова: латунь, усталость, ковка, упрочнение, повреждение.

Introduction. Copper and its alloys submitted to forming processes such as forging and rolling are widely used in various components of sanitary installations (valves, pipe couplings, etc.). The components are often subjected to cyclic loading due to internal pressure variation and impact reaction caused by fluid shock and temperature fluctuation. Therefore, fatigue characteristics are critical for the safe life design of components. The stress-strain behavior of a material after forming process should account for temperature, strain amplitude and hardening–softening rate. Work-hardening behavior also occurs in deformation of metals with different structures [1, 2]. In monotonic deformation, a considerable insight into the effect of microstructure and operating conditions on thermomechanical properties was provided in studies [3–8]. The mechanical behavior and microstructural changes under cyclic deformation were also studied in recent works [9, 10].

El Madhoun et al. [11] have explored the relationship of cyclic deformation behavior with microstructure of materials by means of investigation of stress–strain response and dislocation evolution during low-cycle fatigue. The main effect of grain size was attributed to the cyclic strain hardening. Jia et al. [12] claim that the microscopic substructure developed during cyclic loading is affected by the grain size. In a large grain, strain accommodation occurs in the vicinity of grain boundary. In a smaller grain (20 μm), the dislocation structure evolves in a more

continuous manner by a partial dissolution of the prestrained substructure. Systematic investigation of cyclic deformation behavior of Cu–30 wt.% Zn alloy conducted by Gong et al. [13, 14] has shown that the cyclic deformation behavior is usually dependent on the dislocation structure, its evolution in materials and the strain amplitude applied. The objective of the present study is to evaluate the effect of forging on cyclic stress–strain response and hardening–softening behavior of CW 614 brass alloy. In addition, surface damage was characterized using SEM observation.

1. **Experimental Procedure**. The material under study is a CW 614 brass alloy with the following chemical composition in weight percent: 58.5% Cu, 2.8% Pb, 0.21% Fe, 0.25% Sn, 0.11% Ni, 0.01% Al and the balance Zn. Specimens are obtained from an extruded bar ($3000 \times \varnothing 18$ mm). Tests are carried out on cylindrical specimens with 6 mm diameter and 12 mm gauge length. After machining, the working surface area of the specimen is polished mechanically until a granulometry of 3 μm is reached.

The present work investigated two types of fatigue specimen: (i) specimens manufactured from extruded bar, namely CW 614 and (ii) specimens obtained by severe plastic deformation using forging process, namely CW 614SP. In this process, each specimen is preheated to a temperature within the range of 400–450°C and pressed through a die. In this study, the low-cycle fatigue tests were performed.

Microstructure was examined via optical microscope after etching (using Keller reagent). For CW 614 structure, microscope examination revealed that lightly colored α phase precipitated in the darkly colored β phase matrix (Fig. 1).

Figure 2 shows that the optical microstructure of brass after forging process is characterized by lamellar and ultrafine structure.
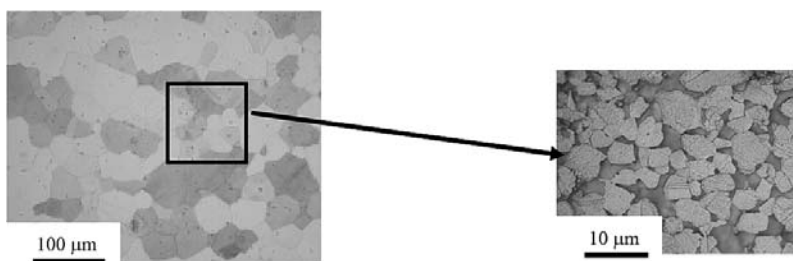

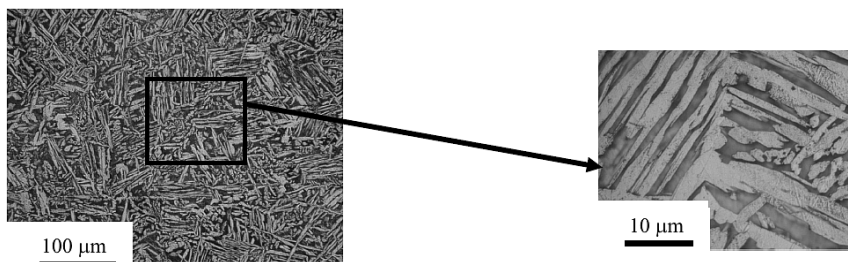Fig. 1. Initial microstructure of CW 614 brass alloy (α/β structure).

Fig. 2. Microstructure of CW 614SP brass alloy after forging process.

In order to understand the forging process effect on mechanical properties, monotonic tensile tests for these two structures of CW 614 alloy were conducted.

The representative stress–strain curves before and after forging process are shown in Fig. 3. As compared to the initial CW 614 structure, the forging process induces a pronounced decrease of both yield stress and flow stress that may be attributed to the consequent substantial grain refinement introduced through forging process leading to modification of the dislocation structure and it evolution in the material.
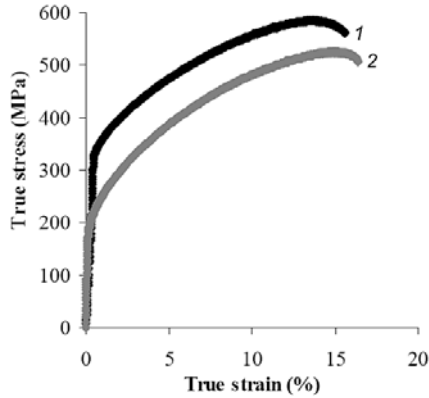

Fig. 3. Monotonic stress–strain curves tested at 25°C [(*1*) CW 614; (*2*) CW 614SP].

Fatigue tests were performed using a servo-hydraulic test machine (Fig. 4) with a symmetrical tensile-compressive loading scheme ($R = -1$) within the temperature range 25 to 200°C and a frequency of 0.1 Hz. A triangular wave signal was used for the total control strain. Strain was measured using a longitudinal extensometer of 10 mm gauge length. During test, the stress values were continually recorded. The stress–strain hysteresis loops were registered by X–Y chart recorder.
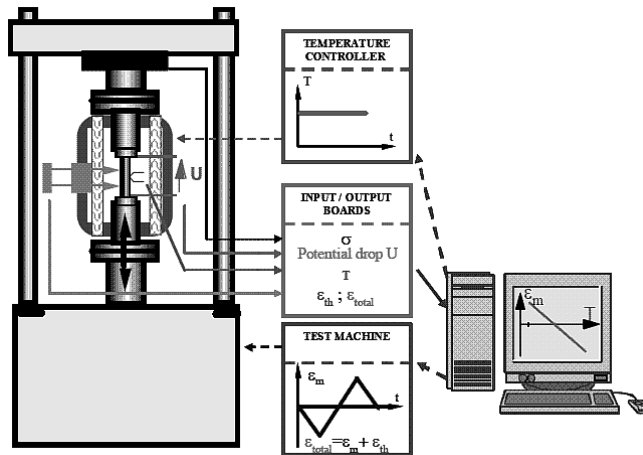

Fig. 4. Thermal mechanical fatigue test [15].

2. **Experimental Results and Discussion**.

2.1. *Cyclic Stress–Strain Response*. Figure 5 shows the typical stress–strain loops recorded at the tenth cycle under two mechanical strains (± 0.3 and $\pm 0.9\%$) for CW 614 and CW 614SP. The main differences between these two structures are the following ones: (i) at the same mechanical strain, the stress level recorded for

the CW 614 structure is lower than that of CW 614SP, while the loop shape changes towards a more opened shape for forged structure; (ii) for high mechanical strain such as $\varepsilon = \pm 0.9\%$, we note that the material exhibits a pronounced visco-plastic character accompanied with small increase in the stress level.
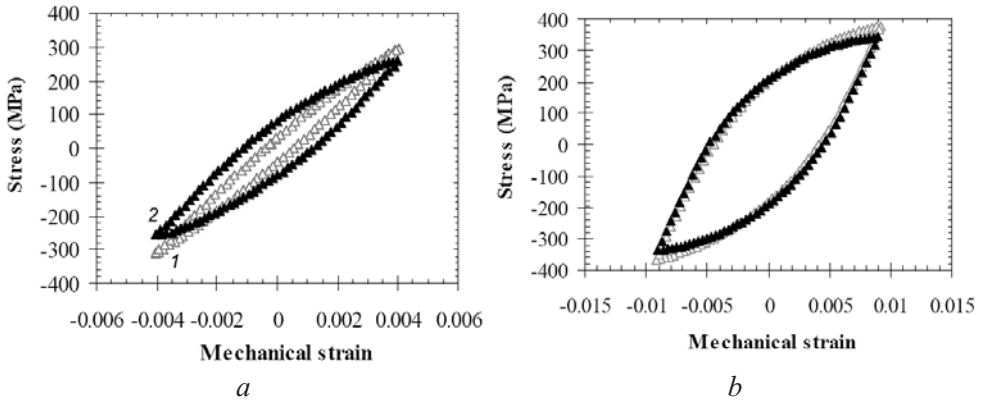

Fig. 5. Mechanical stress–strain loops at tenth cycle in fatigue test ($T = 25°C$, $f = 0.1$ Hz): (*a*) $\varepsilon = \pm 0.3\%$; (*b*) $\varepsilon = \pm 0.9\%$; (*1*) CW 614; (*2*) CW 614SP.

Results are summarized in the form of a cyclic hardening curve as shown in Fig. 6. It was observed that the hardening character is distinguishable in CW 614SP. However, for CW 614 stress saturation was observed (Fig 6a). This mechanical behavior can be attributed to the dislocation arrangement and strain localization in shear bands [16]. In addition, FP specimen exhibits 10% higher saturated flow stress than the initial structure at the same plastic strain amplitude. In contrast to the monotonic test, the yield stress of specimens obtained by forging process was less affected by the cyclic loading (Fig 6b).
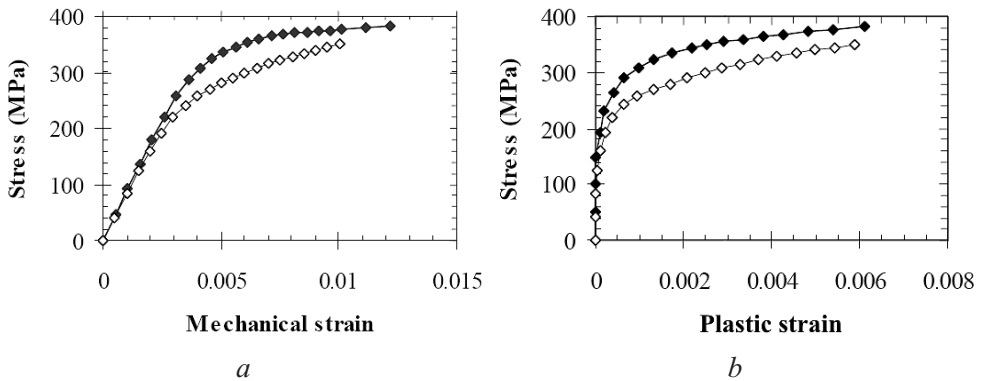

Fig. 6. Cyclic curves of work-hardening: (*a*) according to the mechanical strain; (*b*) according to the plastic strain ($T = 25°C$, $f = 0.1$ Hz); (◆) CW 614; (◇) CW 614SP.

Furthermore, a particular attention was given to characterize the temperature effect in the hardening behavior of CW 614 structure. The effect of temperature on the elastic modulus is shown in Fig. 7 for the CW 614 brass alloy tested at room temperature between 25 and 200°C. For the 25–150°C range, the elastic modulus

decreased gradually as a function of temperature. However, a significant decrease of the elastic modulus is observed when the temperature increases from 150 to 200℃. Therefore, it should be expedient to study the mechanical behavior in the range of transition temperature.
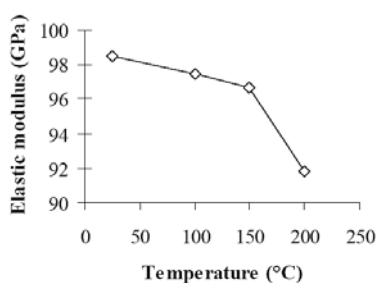

Fig. 7. Elastic modulus evolution as a function of temperature for CW 614.

Figure 8 compares the stress–strain loops recorded at the tenth cycle under two mechanical strains and temperatures (25 and 200℃) for CW 614 structure. We note that the material has an important viscoplastic behavior with wider loops at 200℃.
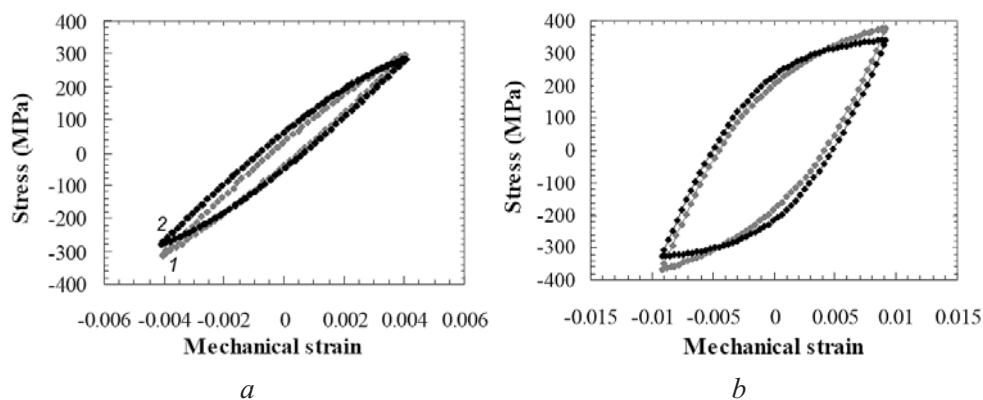

Fig. 8. Mechanical stress–strain loops at tenth cycle in isothermal fatigue test for CW 614 ($f = = 0.1$ Hz): (*a*) $\varepsilon = \pm 0.3\%$; (*b*) $\varepsilon = 0.9\%$; (*1*) $T = 25°C$; (*2*) $T = 200°C$.

Results are summarized in the form of a cyclic hardening curve shown in Fig. 9. In addition to the decrease of the elastic modulus, we observe the decrease of the elastic limit. Nevertheless, the material preserves an important power of hardening at 200℃.

2.2. *Hardening–Softening Behavior.* Figure 10a illustrates the cycling hardening–softening curves for an isothermal test at 200℃. The cyclic response for CW 614SP shows a pronounced cyclic hardening behavior with a hardening rate about 42%. However, for CW 614 structure the cyclic behavior is characterized by an initial strain-hardening after 10 cycles followed by a continuous cyclic softening. The rapid decrease in stress for both structures is attributed to the formation of macroscopic cracks. At the same strain level, we observe that the failure of CW 614 SP specimen occurs after 10,300 cycles, while that of manufactured specimen CW 614 – after 6960 cycles. The cyclic hardening behavior results for CW 614SP

can be attributed to the generation of dislocations and their interaction leading to a continuous decrease in plastic strain as shown in Fig. 10. The difference in fatigue life values therefore has to reflect the effect of forging process on grain boundary which modifies the structure and the evolution of dislocations [17].
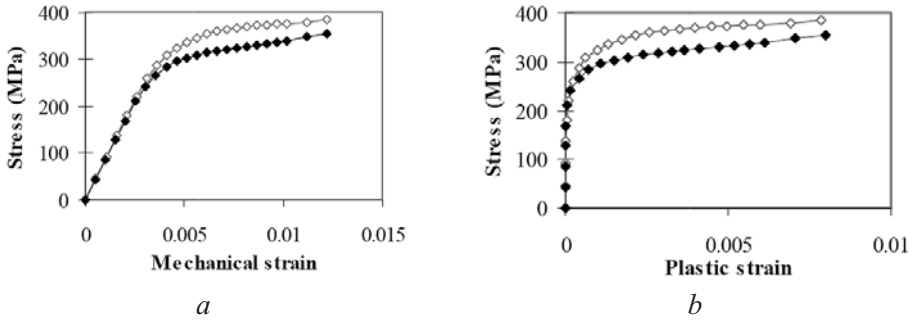

Fig. 9. Cyclic curves of work-hardening: (*a*) mechanical strain; (*b*) plastic strain [($\Diamond$) $T = 25°C$; ($\blacklozenge$) $T = 200°C$; $f = 0.1$ Hz].
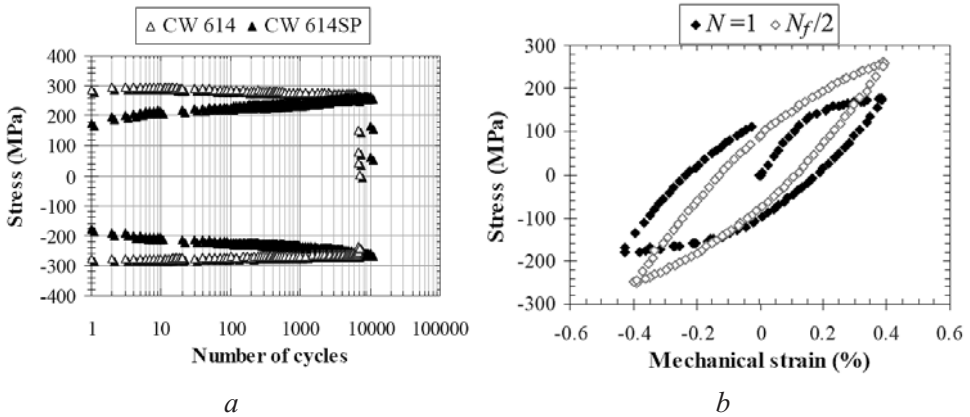

Fig. 10. Hardening–softening curves of isothermal fatigue tests (*a*) and stress–strain loops of the first cycle and half life value (*b*) for CW 614SP ($f = 0.1$ Hz, $\varepsilon = \pm 0.4\%$, $T = 200°C$).

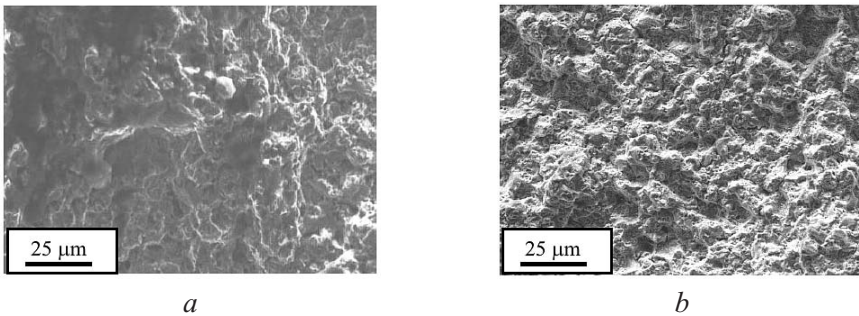Fig. 11. SEM image of fracture surface: (*a*) CW 614 structure and (*b*) CW 614SP structure ($T = 200°C$, $f = 0.1$ Hz, $\varepsilon = \pm 0.4\%$).

2.3. *Damage Analysis*. Surface fracture analysis of specimens cycled at strain amplitude $\varepsilon = \pm 0.4\%$ is shown in Fig. 11. Fracture mechanism for both specimens is due to coalescence of pores observed in the specimen center region and close to

the external surface. In fact, the process of fatigue damage begins by formation of pores or voids and continues by the linking of these pores into embryo cracks which grow inward and slowly propagate leading to fatigue failure. Isolated pockets of shallow dimples are indicative of the ductile nature of failure of the microstructure.

Conclusions. We present results of experimental tests on the cyclic stress–strain response and hardening–softening behavior of CW 614 and CW 614SP alloys.

A difference in stress response to cyclic loading was identified between the original (CW 614) and forged (CW 614SP) structures. Moreover, the hardening pattern is more pronounced in the CW 614SP alloy. A significant decrease of the elastic modulus was observed at 150℃.

In terms of fatigue life, the cyclic behavior is characterized by cyclic hardening for CW 614SP structure. However, a stress stabilization was observed for CW 614. The fatigue life values of CW 614SP structure in isothermal fatigue tests are more higher than those of CW 614.

Р е з ю м е

Проведено дослідження циклічного зміцнення латуні CW 614 на зразках, що виготовлені за двома технологіями: промислова і шляхом кування. Для кожного типу зразка встановлено особливості циклічного зміцнення і циклічної петлі гістерезиса. Представлено результати аналіза процесу руйнування на основі фрактографічних досліджень.

1. C. Mapelli and R. Venturi, "Dependence of the mechanical properties of α/β brass on the microstructural features induced by hot extrusion," *Scripta Mater.*, **54**, 1169–1173 (2006).

2. E. C. S. Correa, M. T. P. Aguilar, and P. R. Cetlin, "The effect of tension/torsion strain path changes on the work hardening of Cu–Zn brass," *J. Mater. Proc. Technol.*, **124**, 384–388 (2002).

3. K. Neishi, T. Uchida, A. Yamauchi, et al., "Low temperature superplasticity in a Cu–Zn–Sn alloy processed by severe plastic deformation," *Mater. Sci. Eng.*, **A307**, 23–28 (2001).

4. D. Y. Li, L. Wang, and W. Li, "Effects of grain size from micro scale to nanoscales on the yields strain of brass under compressive and tensile stresses using a Kelvin probing technique," *Mater. Sci. Eng.*, **A384**, 355–360 (2004).

5. R. Nowosielki, "Ductility minimum temperature in selected mono-phase, binary brasses," *J. Mater. Proc. Technol.*, **109**, 142–153 (2001).

6. K. Neishi, Z. Horita, and T. G. Langdon, "Achieving superplasticity in a Cu–40%Zn alloy trough severe plastic deformation," *Scripta Mater.*, **45**, 965–970 (2001).

7. N. Mostafa, E. Gomaa, and M. Mohsen, "Correlation of thermo-mechanical properties with microstructure in commercial pure Cu an Cu–Zn alloys studied by positron annihilation," *Mater. Sci. Eng.*, **A373**, 250–254 (2004).

8. V. Bursikova, J. Bursik, V. Navratil, and K. Milicka, "Creep behavior of lead brass," *Mater. Sci. Eng*., **A324**, 235–238 (2002).

9. D. Peter, M. Ahmad, and G. B. Ian, "Cyclic response of plate steels under large inelastic strain," *J. Constr. Steel Res*., **63**, 156–164 (2007).

10. Z. Jixi and J. Yanayo, "Fatigue of polycrystalline copper with different grain sizes and texture," *Int. J. Plasticity*, (2005) (in press).

11. Y. El Madhoun, A. Moamed, M. N. Bassim, "Cyclic stress-strain behavior of polycristalline nickel," *Mater. Sci. Eng*., **A385**, 140–147 (2004).

12. W. P. Jia and J. V. Fernandes, "Mechanical behaviour and the evolution of the dislocation structure of copper polycrystal deformed under fatigue/tension and tension/fatigue sequential strain path," *Mater. Sci. Eng*., **A348**, 133–144 (2003).

13. Z. Wang, B. Gong, and Z. G. Wang, "Cyclic deformation behavior of Cu–30wt.% Zn single crystals oriented for single slip. I. Cyclic deformation response and slip band behavior," *Acta Metall*., **47**, 307–315 (1999).

14. B. Gong, Z. Wang, B. Gong, and Z. G. Wang, "Cyclic deformation behavior of Cu–30wt.% Zn single crystals oriented for single slip. II. Dislocations structures," *Acta Metall.*, **47**, 317–324 (1999).

15. A. Koster, E. Fleury, E. Vasseur, and L. Remy, "Thermal mechanical fatigue test," in: ASTM STP 1231 (1994), pp. 559–576.

16. H. L. Huang, "A study of dislocation evolution in polycrystalline copper during low cycle fatigue at low strain amplitudes," *Mater. Sci. Eng*., **A342**, 38–43 (2003).

17. J. V. Carstensen, PhD Thesis, Technical University of Denmark (1998).